

patients with K-L grade 4 of knee deformity ($p=0.012$) and diabetes ($p=0.003$) presented higher porous SP. Those with essential hypertension presented lower BMD of SP ($r^2=0.635$, $p<0.001$).

Conclusions: This study firstly unveiled the interplay of localized knee deformity based on x-radiography using K-L grading system, preoperative Knee Society score and Functional Scales and systemic disorders, i.e. diabetes and essential hypertension, in end stage of knee OA, in terms of their contributions to the subchondral bone disturbance.

446

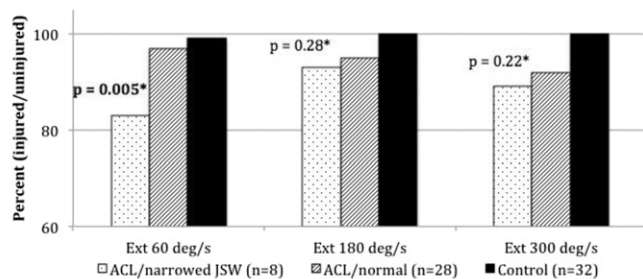
RELATIONSHIP BETWEEN ISOKINETIC STRENGTH AND TIBIOFEMORAL JOINT SPACE WIDTH CHANGES FOLLOWING ACL RECONSTRUCTION

T.W. Tourville, K.M. Jarrell, S. Naud, R.J. Johnson, B.D. Beynnon. Univ. of Vermont Coll. of Med., Burlington, VT, USA

Purpose: Following anterior cruciate ligament (ACL) injury and reconstruction (ACL-R), quadriceps muscle weakness and low hamstring-to-quadriceps muscle strength ratios have been associated with post-traumatic osteoarthritis (PTOA) as well as primary OA. However, this relationship has not been examined using tibiofemoral joint space width difference (JSW-D) as a measurement of PTOA onset. JSW-D is a measurement technique that is sensitive to PTOA changes prior to the clinical manifestation of the disease. It is important to determine risk factors associated with the onset and progression of PTOA at the earliest time point in the disease process when intervention can alter the progression of the disease. Consequently, the focus of this study was to examine the relationship between isokinetic knee strength and JSW-D at one and four years post-ACL-R compared to a group of healthy, non-injured subjects of similar sex, age, BMI, and activity level.

Methods: A secondary analysis of data collected during a longitudinal study of biomarkers of PTOA following ACL-R was utilized for this exploratory study. Entry criteria for injured subjects included: age at time of ACL-R = 14-55; BMI = 18.5-30; Tegner activity score > 4 ; $< 2/3$ meniscectomy; $<$ grade IIIa articular cartilage lesions; no history of joint surgeries, knee injections, or other knee pathologies; no abnormal knee laxity or evidence of radiographic OA at baseline. Additional criteria for controls included: no knee pain/dysfunction, and normal clinical evaluation and baseline MRI. At 1- and 4-years post ACL-R, standing, bilateral metatarsal phalangeal (MTP) view knee x-rays were obtained for JSW assessment. Subjects were considered to have significant narrowing if their injured minus normal (contralateral) knee JSW difference (JSW-D) fell below the 95% confidence interval of controls. At the same time point, isokinetic knee strength was assessed at 60, 180, and 300 deg/sec, and normalized to body weight. Relationships between strength and JSW-D were evaluated between ACL subgroups (normal and narrowed) and controls using analysis of covariance adjusted for age, sex, BMI, and time since surgery. Post-hoc group comparisons were made using Fisher's LSD.

Results: Of the 34 ACL-R patients included, 6 had significant JSW-D narrowing at 1-year follow-up, and 8 had narrowing at 4-year follow-up. The mean strength values for all ACL-R subjects ("normal" and "narrowed JSW-D" groups combined) were found to be significantly less than the control group at both time points. However, ACL-R subjects with narrowed JSW-D did not differ from normal JSW-D subjects (all $p > 0.20$) with one exception: extension at 60 degrees/second at four-year follow-up ($p = 0.005$). The pattern of knee extension strength at 60 deg/sec at 1-year follow-up was similar to changes observed at 4-year follow-up. Extension to flexion strength ratios were not found to have a significant association with JSW-D at any speed.



*p-values represent difference between ACL normal JSW-D and ACL narrowed JSW-D groups

Figure 1. Isokinetic extension peak torque at final follow-up.

Conclusions: Strength deficits present as early as one year following ACL-R and persist at 4-years post. In general, ACL-R group subjects were not found to have significantly different strength values within JSW subgroups. In contrast to previous studies, the current investigation did not reveal an association between PTOA and low extension to flexion strength ratios. It should be noted that no subjects in this study reported appreciable pain/dysfunction or reduced physical activity, which is indicative of the clinical manifestation of OA. However, subjects with narrowed JSW-D had significantly lower extension strength at 60 degrees/second than controls and injured subjects with normal JSW-D. It may be that individuals that loose a significant amount of knee extension strength are at greater risk for tibiofemoral JSW narrowing following ACL trauma.

447

TIBIOFEMORAL CONTACT AREA REMAINS ABNORMAL FOLLOWING ANTERIOR CRUCIATE LIGAMENT RECONSTRUCTION

D.A. Lansdown, C.R. Allen, S. Wu, L.J. Morse, W. Schairer, X. Li, B. Ma. Univ. of California, San Francisco, San Francisco, CA, USA

Purpose: Injury to the anterior cruciate ligament is highly prevalent, especially in active populations, with approximately 90,000 ACL ruptures in the U.S. each year. The cartilage contact points are significantly changed in the ACL deficient state, and degenerative changes develop in 82-89% of these patients. The goal of ACL reconstruction is to stabilize the knee and restore normal cartilage contact. Multiple operative techniques are utilized for ACL reconstruction, including the mini-two incision (MT) technique and the anteromedial portal (AM) method. There have been no prior reports to our knowledge regarding the in vivo contact areas after MT reconstruction. We hypothesized that both the MT and AM techniques would result in cartilage contact area that was not significantly different from the patient's contralateral knee.

Methods: Seven patients (4 female; average 15.5 months post-operative) with MT reconstruction and 12 patients (7 female; 12 months post-operative) with AM reconstruction underwent kinematic MR imaging. T2-weighted sagittal images were obtained of the reconstructed and uninjured knee in extension and 30 degrees of flexion with an applied load of 125 N. Cartilage contact areas were manually segmented using in-house Matlab software. The defined Bezier splines were connected with triangles, and the contact area was defined as the summation of the area of the triangles (Figure 1). The contact centroid was defined as the centroid of the triangles. Statistical analyses were performed with a paired t-test with alpha of 0.05 for comparisons of each patient to the contralateral knee.

Results: The contact area (Figure 1) of the medial compartment was significantly lower in MT reconstruction compared to the uninjured side at 90.1% (standard deviation 4.8%) in extension ($p=0.003$) and 86.3% (7.3%) in flexion ($p=0.004$). For AM reconstruction, the only significant change was in the lateral compartment in flexion, which was higher in the reconstructed knee at 111% (18.9%) ($p=0.03$). With the MT reconstruction, the medial contact centroid shifted laterally by 9.5 mm in extension ($p=0.05$) and 10.2 mm in flexion ($p=0.02$) between the reconstructed and contralateral knees. In knees with AM reconstruction, the lateral contact centroid shifted anteriorly by 3.5 mm in extension ($p=0.05$) and the by 4.4 mm ($p=0.03$) in flexion as compared to the normal knee.

Conclusions: The MT technique results in partial restoration of medial compartment articular cartilage area. Additionally, the medial contact centroid is shifted laterally in the MT reconstructed knees. The AM reconstructed knees showed a significant change in the medial and lateral contact centroids in extension. The cartilage contact area was more closely restored in the patients with AM reconstruction. Morimoto et al showed significantly decreased medial and lateral contact areas in single bundle ACL reconstructions. Li et al demonstrated a posterior and lateral shift of the medial contact centroid in ACL deficient knees. Persistent changes in cartilage contact area may contribute to early degenerative changes. Our results suggest that the AM technique may offer improved restoration of cartilage contact areas versus the MT technique, though persistent changes in contact area and centroid location remain with both techniques.

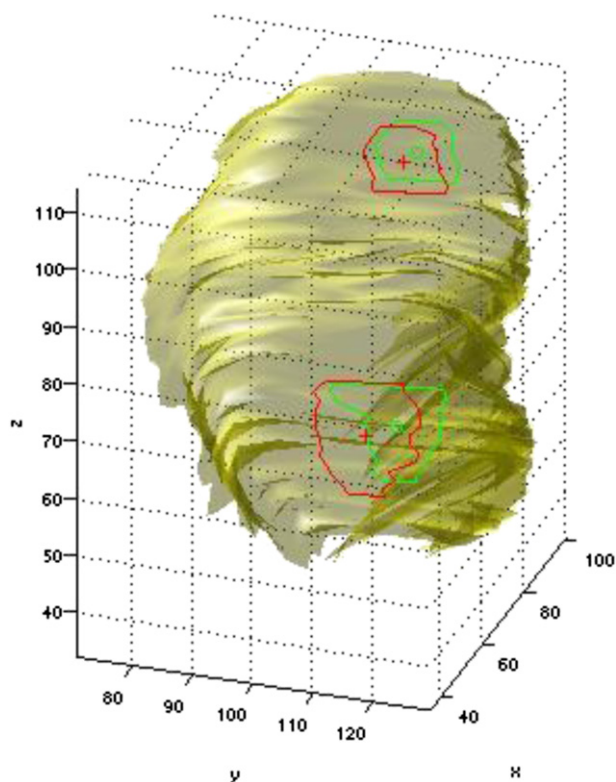


Figure 1. Relative contact area of reconstructed knees as compared to contralateral controls.

448 IS CARTILAGE AND SUBCHONDRAL BONE COVERED BY MENISCI WEAK

H. Iijima[†], T. Aoyama[‡], A. Ito[†], J. Tajino[†], M. Nagai[†], X. Zhang[†], S. Yamaguchi[†], H. Akiyama[§], H. Kuroki[†]. [†]Dept. of Motor Function Analysis, Graduate Sch. of Med., Kyoto Univ., Kyoto, Japan; [‡]Dept. of Dev. and Rehabilitation of Motor Function, Graduate Sch. of Med., Kyoto Univ., Kyoto, Japan; [§]Dept. of Orthopaedic Surgery, Graduate Sch. of Med., Kyoto Univ., Kyoto, Japan

Purpose: Cartilage that is uncovered by menisci usually bears the body weight in intact knee. However it has been suggested that structural change of the knee due to meniscectomy leads to alternation of contact regions. The mechanical properties of cartilage and subchondral bone may vary according to the regions covered and uncovered by menisci and the covered regions by menisci may be more susceptible to extreme mechanical stress after meniscectomy. However few studies have focused on the difference of mechanical property of cartilage and subchondral bone architecture between the regions covered and uncovered by menisci. The purpose of this study is to investigate the mechanical and histological properties of cartilage and subchondral bone architecture that may differ between the covered and uncovered regions.

Methods: Articular cartilage was obtained from the 5 porcine knees. After the knee joints were opened, osteochondral plugs (full-depth thickness 2mm) were obtained from tibial cartilage which were covered and uncovered region by menisci. Only sites with a macroscopically normal articular cartilage were included in this study. From one plugs of each regions, cartilage thickness was determined as the average of four sides of plugs. After that, unconfined compression was applied using a mechanical testing instrument (Autograph AG-X, Shimadzu, Japan). Each sample was compressed uniaxially in a testing chamber filled with PBS at room temperature. After surface contact, a pre-load of 0.01N was applied and allowed to equilibrate for 10 minutes. Then, loading was applied at a strain rate of 0.001mm/s up to 20% strain and hold for 30 minutes. Three features were extracted from

these curves: the Young's modulus, the peak stress, the relaxation time which was defined as the time for force to decrease to 37% of peak stress. As to the another plugs of each area, a high-resolution micro-CT scanner (SMX-100CT, Shimadzu, Japan) was used to determine structural parameters of the subchondral bone of the medial and lateral tibial plateau under the covered region and uncovered region. The measurement regions were 200µm in height in columnar region located 1mm beneath the osteochondral junction. All structural analyses were based on the 3D image data sets using software (Amira5.4, Visage, Germany). Bone volume ratio (BV/TV) and trabecular thickness (Tb.Th) were calculated based on the 3D data. After that the 6µm thick sections were made and collagen amount was observed by integral calculus of Amide-I area using Fourier-transform infrared imaging (IRT-5000, FT/IR-4100, JASCO, Japan). Further, the sections were stained with SafraninO-Fast green staining to assess glycosaminoglycan (GAG) content, Hematoxylin-Eosin for morphological measurement and Picrosirius red for collagen orientation measurement by using polarizing microscope.

Results: The average cartilage thickness of each area was significantly larger in medial and lateral uncovered regions ($P < 0.05$). Both Young's modulus and peak stress were significantly greater in medial and lateral covered regions ($P < 0.05$), while relaxation time for force to decrease to 37% was shorter in medial and lateral covered regions ($P < 0.05$). The subchondral trabecular showed BV/TV and Tb. Th were significantly larger in uncovered regions ($P < 0.05$). The integral calculus of Amide-I area was significantly higher in uncovered regions. Safranin O staining revealed that much proteoglycan was confirmed in medial and lateral uncovered regions. Picrosirius red staining revealed that superficial zone and middle zone showed brightly in uncovered regions, while deep zone showed brightly in covered regions.

Conclusions: Our results revealed a difference of the mechanical properties and structures of articular cartilage and subchondral bone between the regions covered and uncovered by menisci.

449 FULLY-AUTOMATED CARTILAGE SEGMENTATION FROM MAGNETIC RESONANCE IMAGES OF THE KNEE USING ATLAS AND GRAPH-CUT ALGORITHMS

J.-G. Lee, S. Gumus, K.C. Kwoh, K.T. Bae. Univ. of Pittsburgh Sch. of Med., Pittsburgh, PA, USA

Purpose: To develop fully automated method to segment cartilage from magnetic resonance (MR) images of the knee and evaluate the performance on public open dataset.

Materials and Methods: 100 cases of MR images from public open dataset (available at www.ski10.org) were used for this study. The MR images were acquired at multi-centers and multi-vendor machines. All images were acquired in the sagittal plane with a pixel spacing of 0.4*0.4mm and a slice distance of 1mm. MR Field strength was 1.5 T in about 90% of the cases, the rest was acquired 3T and 1T. The vast majority of images were scanned by gradient echo based T1-weighting MRI sequence with fat suppression. After acquisition, all images were segmented interactively by experts at Biomet, Inc. to label and delineate the bone and cartilage of the femur and tibia. Each case from the dataset was available with original MR images and the corresponding segmentation mask to form the ground truth segmentation result. We divided total 100 cases into training set (60 cases) and test set (40 cases).

The segmentation scheme was composed of two procedures, atlas building and local adjustment. In the atlas building procedure, all training cases were registered to the given test case by non-rigid registration scheme. The final metric values from each registration were recorded for sorting. Nine best matched results were selected and merged to generate the atlas based segmentation mask. In the local adjustment procedure, the statistical information of bone, cartilage and surrounding regions was computed from the atlas based segmentation result. We incorporated a graph-cut based method for local adjustment. Firstly, the inside and outside seed points were selected from the statistical information and the bone regions were identified by the graph-cut based method. Secondly, distance and intensity based probability maps were generated and used as weighting factor in calculating capacity values. The inside and outside seed points for cartilage were